

# Dynamic Finite-Element Analysis of Jointed Concrete Pavements

KARIM CHATTI, JOHN LYSMER, AND CARL L. MONISMITH

A new dynamic finite-element computer program, DYNA-SLAB, for the analysis of jointed concrete pavements subjected to moving transient loads is presented. The dynamic solution is formulated in both the time and the frequency domains. The structural model for the slab system is the one used in the static computer program ILLI-SLAB. The foundation support is represented by either a damped Winkler model with uniformly distributed frequency-dependent springs and dashpots or a system of semi-infinite horizontal layers resting on a rigid base or a semi-infinite half-space. An important contribution from the study is a new analytical method for determining the stiffness and damping coefficients to be used in the Winkler foundation model. The accuracy of DYNA-SLAB has been verified by comparing the results produced by the program with those from theoretical closed-form solutions and from a powerful dynamic soil-structure interaction computer program called SASSI as well as with field data. The analytical results indicate that dynamic analysis is generally not needed for the design of rigid pavements and that it usually leads to decreased pavement response. Thus, it appears that a quasistatic analysis is sufficient and that the results from this type of analysis will generally be conservative, provided that the wheel loads used in the analysis have been adjusted for the effects of vehicle velocity, truck suspension characteristics, and pavement roughness.

The problem of truck-pavement dynamics and its importance in the analysis and design of rigid pavements has been an increasing concern in the field of pavement engineering in recent years. The questions of (a) how important dynamic considerations are in affecting rigid pavement response and (b) which characteristics of the truck-pavement system are the most significant are yet to be answered. Today there are a number of finite-element methods available for analyzing jointed concrete pavements (1-5). However, these methods are restricted to static analysis. Recently, a few dynamic methods have been presented (6-8). These new methods are, however, confined to the analysis of continuous flexible pavements. A dynamic finite-element method for rigid airport pavements has just been published (9). The method, however, is not directly suited for incorporating realistic truck loads. Furthermore, the method is limited to representing the subgrade by a standard damped Winkler foundation.

This paper presents a new dynamic method for analyzing jointed concrete pavements subjected to moving dynamic truck loads. These loads are obtained by using truck simulation programs and are subsequently introduced to the pavement model as transient loads with arbitrary time histories. The method, which was implemented in a computer program called DYNA-SLAB, is an improvement over state-of-the-art procedures because it allows

for moving transient loads and uses improved foundation support models. An additional important contribution from this study is a new analytical method for determining the stiffness and damping coefficients to be used in the Winkler foundation model.

The paper first describes the models and methods of analysis used in DYNA-SLAB. Later, an attempt to answer the questions raised above is made through the use of some application examples.

## DESCRIPTION OF MODEL

### Structural Model

The structural model for the concrete slab system and load transfer mechanisms used in DYNA-SLAB is a modification of the model used in the well-known computer program ILLI-SLAB (3). The modified program accounts for inertial and viscous effects. In brief, the concrete slab is modeled by rectangular medium-thick plate elements that were independently developed by Melosh (10) and Zienkiewicz and Cheung (11). Each node contains three degrees of freedom: A vertical translation in the  $z$ -direction and two rotations about the  $x$  and  $y$  axes, respectively. Load transfer across joints is modeled either by a vertical spring element, to represent aggregate interlock or keyway, or by a bar element, to represent dowel bars. ILLI-SLAB's capability of handling the effects of stabilized bases or overlays on the stresses and deflections in concrete pavements, among other features, has been maintained. A description of the static model has been given previously (3). Figure 1 shows a schematic view of the DYNA-SLAB model.

### Foundation Support Models

The subgrade is modeled by either a damped Winkler foundation with frequency-dependent springs and dashpots, uniformly distributed underneath the slabs, or a viscoelastic layered system on a rigid or deformable half-space.

In the Winkler foundation option the values for the springs ( $k$ ) and dashpots ( $c$ ) are determined by equating elastic and viscous forces, respectively, from steady-state force-displacement relationships of a massless slab supported by a layered medium and subjected to a harmonic unit load. To the best of the authors' knowledge, this method is the first attempt to determine the values of  $k$  and  $c$  analytically. The method is described next.

In the layered-solid foundation option, the subgrade dynamic stiffness matrix is obtained by inverting the dynamic flexibility matrix corresponding to the layered medium (Figure 2). At each frequency the  $i$ th non-zero column of the flexibility matrix is

K. Chatti, Department of Civil and Environmental Engineering, A349 Engineering Building, Michigan State University, East Lansing, Mich. 48824. J. Lysmer, Department of Civil Engineering, University of California, Berkeley, 400 Davis Hall, Berkeley, Calif. 94720. C. L. Monismith, Institute of Transportation Studies, Department of Civil Engineering, University of California, Berkeley, 215 McLaughlin Hall, Berkeley, Calif. 94720.

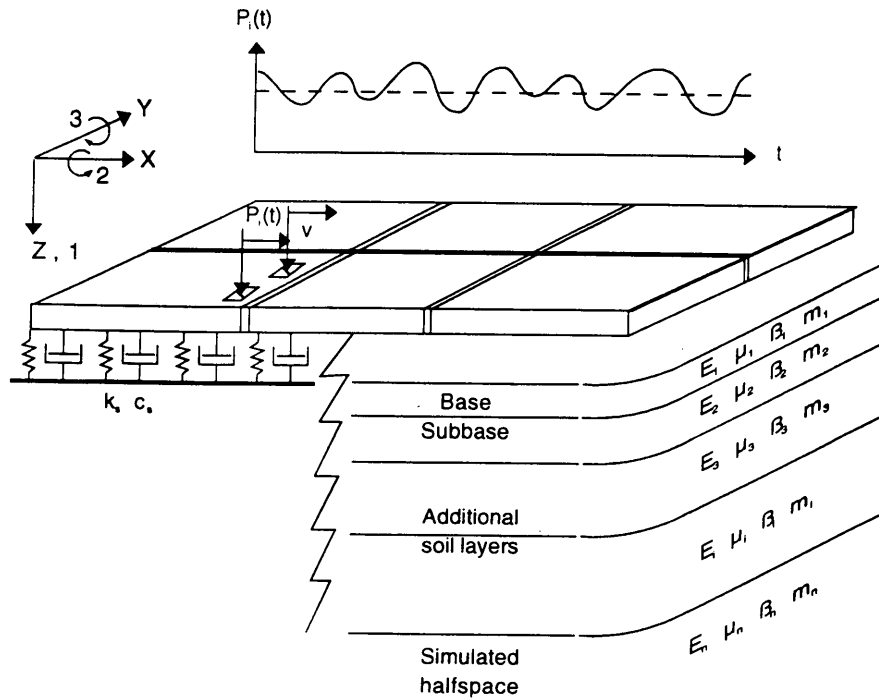


FIGURE 1 Schematic view of the DYNA-SLAB model, with damped Winkler foundation (LHS) and layered solid foundation (RHS).

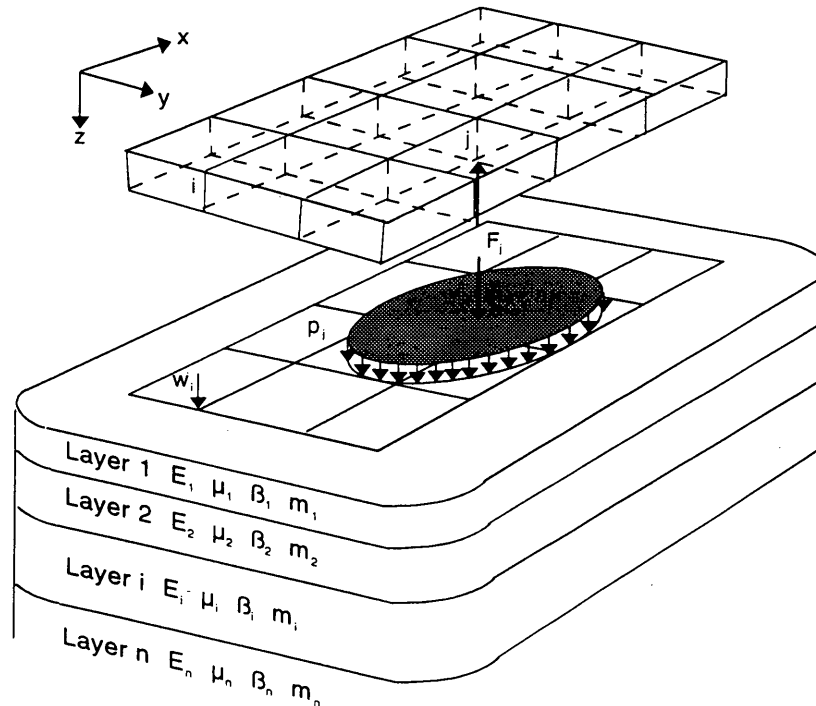


FIGURE 2 Interaction between concrete slab and multilayered system.

formed by calculating the vertical (complex) displacements, at all nodes, because of a vertical harmonic disk load of unit amplitude acting at Node *i*. The radius of the disk load is chosen equal to the distance between two adjacent nodes to establish compatibility with plate element displacements.

For both foundation types the displacement basin underneath the slab system is computed by using a computer program called SAPSI, developed at the University of California, Berkeley (6). This program solves for the response of a layered medium subjected to stationary dynamic surface disk loads. The accuracy of the SAPSI program has been verified by using available "exact" solutions (6) and more recently by comparing SAPSI results with extensive field data obtained using nondestructive test equipment for airfield pavements (12).

**Method for Determining Dynamic Subgrade Stiffness and Damping Coefficients**

Consider a massless slab resting on a layered soil profile over a half-space or a rigid boundary. If the layered foundation is equated to an analog system consisting of distributed springs and dashpots, then the internal forces in the system will be the elastic and viscous forces, which are represented by the springs, *k*, and the dashpots, *c*, respectively. The inertial forces in the slab are zero since the slab is massless. The only external force is the exciting force (Figure 3). The dynamic equilibrium of the system is satisfied by the following equation:

$$P(t) = k \int_A u(r,t)dA + c \int_A \dot{u}(r,t)dA \quad (1)$$

where *k* and *c* are the real elastic and viscous forces, averaged over the displaced volume, respectively, and the integrals represent the volume of the displacement basin, or its time derivative. For the steady-state case with circular frequency  $\omega$ , the exciting force and the displacement response are both harmonics. By substituting these into Equation 1, equating the real and imaginary parts separately, and solving for *k* and *c*, one obtains (13):

$$k = P_0 \cdot \frac{\int_A ReU dA}{\left(\int_A ReU dA\right)^2 + \left(\int_A ImU dA\right)^2} \quad (2)$$

$$c = -\frac{P_0}{\omega} \cdot \frac{\int_A ImU dA}{\left(\int_A ImU dA\right)^2 + \left(\int_A ReU dA\right)^2}$$

These expressions will not work for edge/corner loadings.

**Moving Load Representation**

A moving load is represented by using local displacement shape functions from the finite-element formulation at successive time-dependent positions of the load as it moves from one plate element to the next. Thus, at each instant of time the global load vector is composed of zero entries except at the nodes of those elements on which the load is positioned. This block of nonzero values will

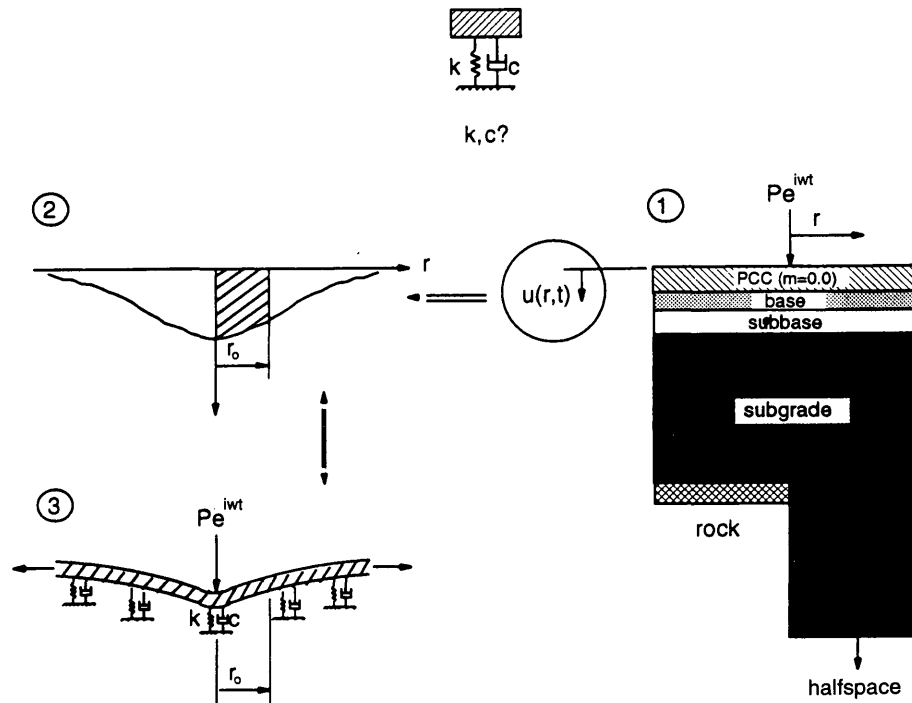


FIGURE 3 Determination of foundation parameters *k* and *c*.

be moving to other parts of the load vector as the load moves along the slab system. For a load distributed over a small area within an element, the block of nonzero values is composed of equivalent nodal forces expressed by

$$\{\bar{P}\}_e = \int_{b_1}^{b_2} \int_{a_1(t)}^{a_2(t)} [N(x,y)]^T p(t) dx dy \quad (3)$$

where

$$a_1(t) = [v_0 t - (a/2)],$$

$$a_2(t) = [v_0 t + (a/2)],$$

$[N]$  = shape function matrix for the element on which the distributed load is acting,

$b_1$  and  $b_2$  = constant local  $y$ -limits of the loaded area,

$a_1(t)$  and  $a_2(t)$  = local  $x$ -limits of the loaded area, and

$a$  = length of the loaded area.

For multiple loads the overall load vector is obtained by superposing the effects of the individual loads.

## METHOD OF ANALYSIS

The equation of motion governing the linear dynamic response of the pavement system is

$$[M]\{\ddot{U}\} + [C]\{\dot{U}\} + [K]\{U\} = \{P(t)\} \quad (4)$$

where  $\{U\}$  is the vector of nodal displacements and  $\{P(t)\}$  is the external load vector acting at the nodal points.  $[M]$ ,  $[C]$ , and  $[K]$  are the total mass, damping, and stiffness matrices, respectively. The stiffness and damping matrices include the contributions from the slab system and the subgrade. The matrices for both stiffness and damping of the subgrade are based on the consistent mass formulation. The matrices can be written as

$$[M] = \sum_{e=1}^n [M]_e = \sum_{e=1}^n \rho_e \iint_{A_e} [N]_e^T [N]_e dA_e \quad (5)$$

$$[K] = \sum_{e=1}^n ([K]_{\text{plate}} + [K]_{\text{subgrade}})_e \\ = \sum_{e=1}^n \left( \iint_{A_e} [B]_e^T [D]_e [B]_e dA_e + k_e \iint_{A_e} [N]_e^T [N]_e dA_e \right) \quad (6)$$

$$[C] = \sum_{e=1}^n [C]_{\text{subgrade}_e} = \sum_{e=1}^n c_e \iint_{A_e} [N]_e^T [N]_e dA_e \quad (7)$$

where

$[N]_e$  = element shape function matrix,

$[B]_e$  = operator matrix expressing strains as a function of displacements, and

$[D]_e$  = constitutive matrix expressing stresses as a function of strains.

In the frequency-domain solution damping can be conveniently introduced by the use of complex stiffness matrices, which are formed exactly like real-valued matrices  $[K]$  except that real coefficients are replaced by the corresponding complex values.

Two methods were used to solve the equation of motion (Equation 4), depending on the foundation support model. For the frequency-independent Winkler foundation, Newmark's constant acceleration method was chosen among the different time integration methods because the procedure is unconditionally stable and does not introduce artificial numerical damping (14). The method is based on satisfying the equation of motion at successive discrete time points that define a solution time interval,  $\Delta t$ , and assuming the acceleration to be constant within  $\Delta t$  and equal to the average of the end values. The complete algorithm is given elsewhere (14).

For both the frequency-dependent Winkler and the layered system foundations the complex response method was used. This method uses a complex representation for harmonic oscillations to solve for the steady-state response at several frequencies and obtains the transient response by superposition by using Fourier transforms. A more complete discussion of the complex response method can be found elsewhere (15).

## VERIFICATION

To verify the moving load algorithm, DYNA-SLAB results were compared with the results obtained from two limiting theoretical solutions:

1. An approximate solution for the case of a point load moving on an infinite plate supported by an elastic Winkler foundation (16). The solution, which assumes that the displacement depends only on the radial variable, is valid only at speeds less than approximately half the critical speed of wave propagation (the velocity of flexural waves in the slab). As shown in Figure 4(a), good agreement was observed within the range of validity of the approximate solution.

2. An exact solution for the case of a transient load moving on a beam of finite length supported by a viscoelastic Winkler foundation (13,17). As shown in Figure 4(b), DYNA-SLAB predictions agree closely with this "closed-form" solution.

To verify the foundation models, deflection amplitudes due to harmonic loading for both interior and edge load cases were calculated at several frequencies by using DYNA-SLAB, with both foundation models, and compared with the results obtained by using a powerful three-dimensional dynamic soil-structure interaction computer program called SASSI (15) for three different soil profiles: a "typical" layered pavement profile [Figure 5(a)], a weak homogeneous half-space [Figure 5(b)], and a strong soil layer resting on a stiff rock formation [Figure 5(c)]. The values of  $k$  and  $c$  were calculated by the new method described above. The results show that sites with deep soil profiles will exhibit very strong damping ( $\beta > 2.0$ ) because of the dissipation of energy through wave propagation (radiation or geometric damping). This observation is significant because it confirms analytically what several researchers have observed in field measurements of pavement deflections (8,18). Furthermore, the values of  $\beta$  obtained analytically herein fall within the range of values that these same researchers had to use to fit field measurements to theory.

Figures 6 to 8 show that DYNA-SLAB gives excellent results for all cases when the layered foundation system is coupled with the slab system. When the damped Winkler foundation is used there is very good agreement for center deflections; this further verifies the proposed method for determining  $k$  and  $c$ . However,

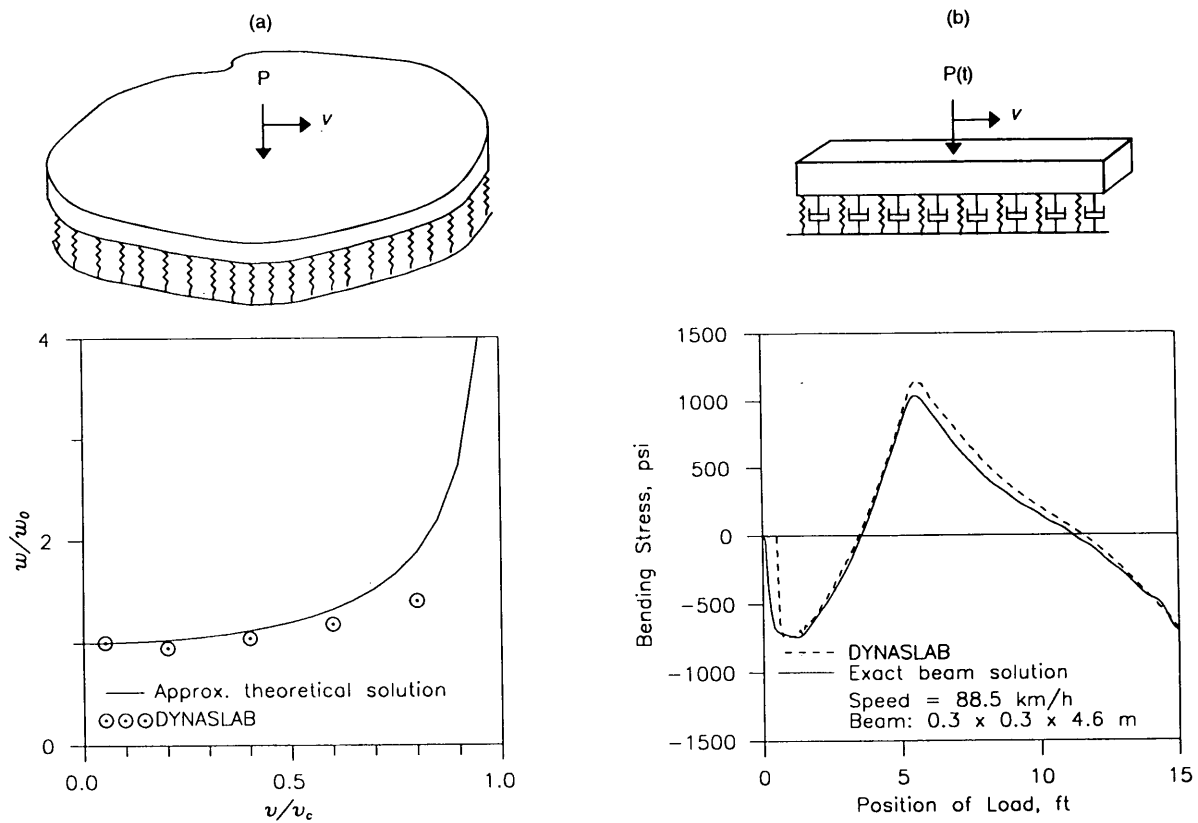
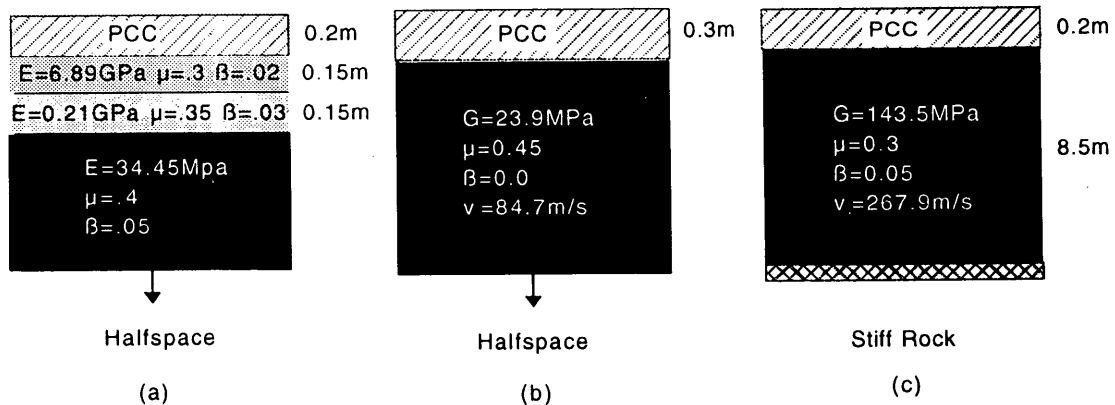


**FIGURE 4** Theoretical verification of DYNA-SLAB: (a) comparison of dynamic to static deflection ratios of an infinite plate on a Winkler foundation; (b) comparison of bending stress influence lines for a finite beam on a damped Winkler foundation.



1 GPa = 103 MPa = 106 kPa ; 1 kPa = 0.145 psi ; 1 m = 3.279 ft

**FIGURE 5** Pavement profiles used in the verification of DYNA-SLAB foundation models: (a) Profile 1; (b) Profile 2; (c) Profile 3.

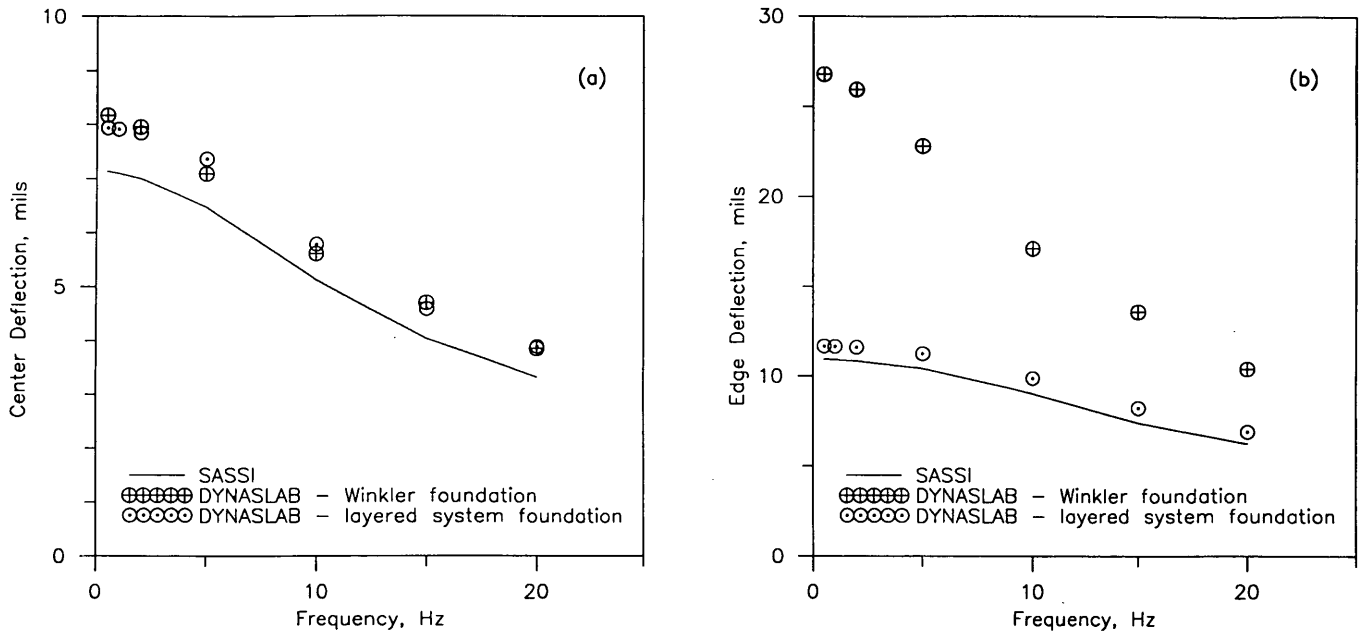


FIGURE 6 Verification of foundation models for Profile 1: (a) center loading; (b) edge loading.

edge deflections that are too high are predicted by DYNA-SLAB when the Winkler foundation is used. This is especially so at lower frequencies. This error is due to the Winkler assumption that implies that soil elements beyond slab edges do not provide any support. Overpredictions also occurred in the case in which there was a stiff layer at a relatively shallow depth (Figure 8). This is because a shallow rigid base may cause a wider deflection basin, suggesting that use of the equivalent radius of the slab as the radius of the deflection basin to compute  $k$  and  $c$  may not be

appropriate in this case. Much better agreement was obtained when the equivalent radius of a rigid slab was used (13).

Further verification of the accuracy of DYNA-SLAB was made by using experimental results from a study conducted by the U.S. Army Corps of Engineers. The purpose of that study was to evaluate a number of nondestructive testing devices for use in airfield pavements (19). Results from three of the four rigid pavement sites (Sites 3, 7, and 11) measured by the WES 16-kip Vibrator were compared with DYNA-SLAB predictions. The results,

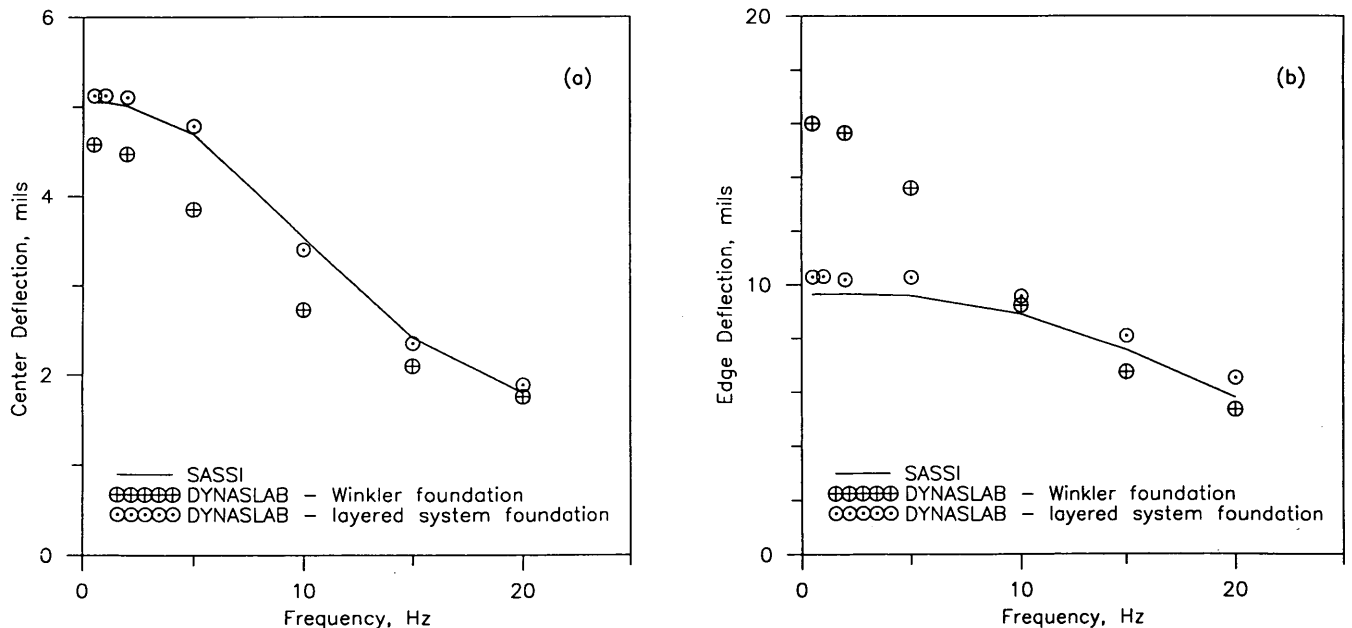


FIGURE 7 Verification of foundation models for Profile 2: (a) center loading; (b) edge loading.

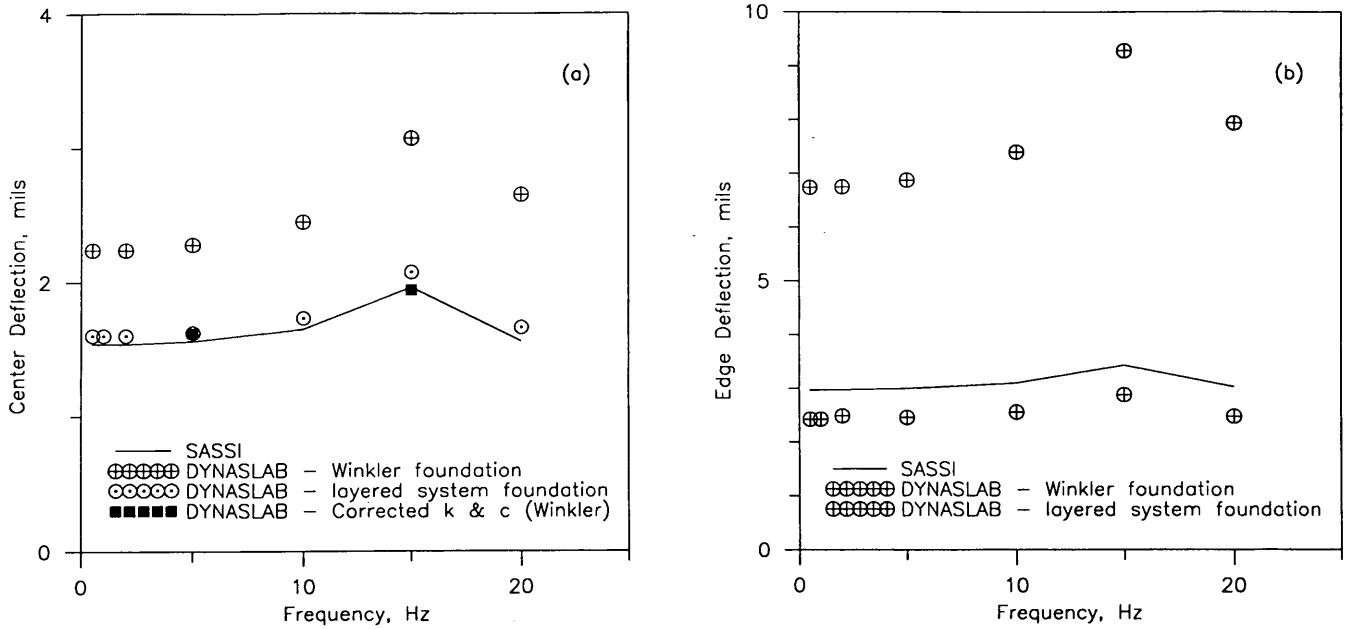


FIGURE 8 Verification of foundation models for Profile 3: (a) center loading; (b) edge loading.

shown in Table 1, indicate that DYNA-SLAB predicts very well the dynamic deflection at the joint, whereas the static ILLI-SLAB agrees well only for the case when the foundation support is stiff [81.4 MPa/m (300 pci) for Site 3 versus 21.7 MPa/m (80 pci) for Sites 7 and 11]. The discrepancy is probably due to a poor choice of the static coefficient of subgrade reaction as well as to the fact that the frequency of interest (15 Hz) departs considerably from the static case (0 Hz). Thus, dynamic effects may be significant.

**PRACTICAL CONSIDERATIONS**

The possible applications of DYNA-SLAB are numerous since it extends all of the capabilities of the original static ILLI-SLAB

into the dynamic range. In the present study, however, the new computer program was used mainly to investigate whether dynamic analysis is really needed to predict the response of jointed concrete pavements subjected to moving dynamic truck loads. This was done through the use of some numerical examples.

**Effects of Vehicle Speed**

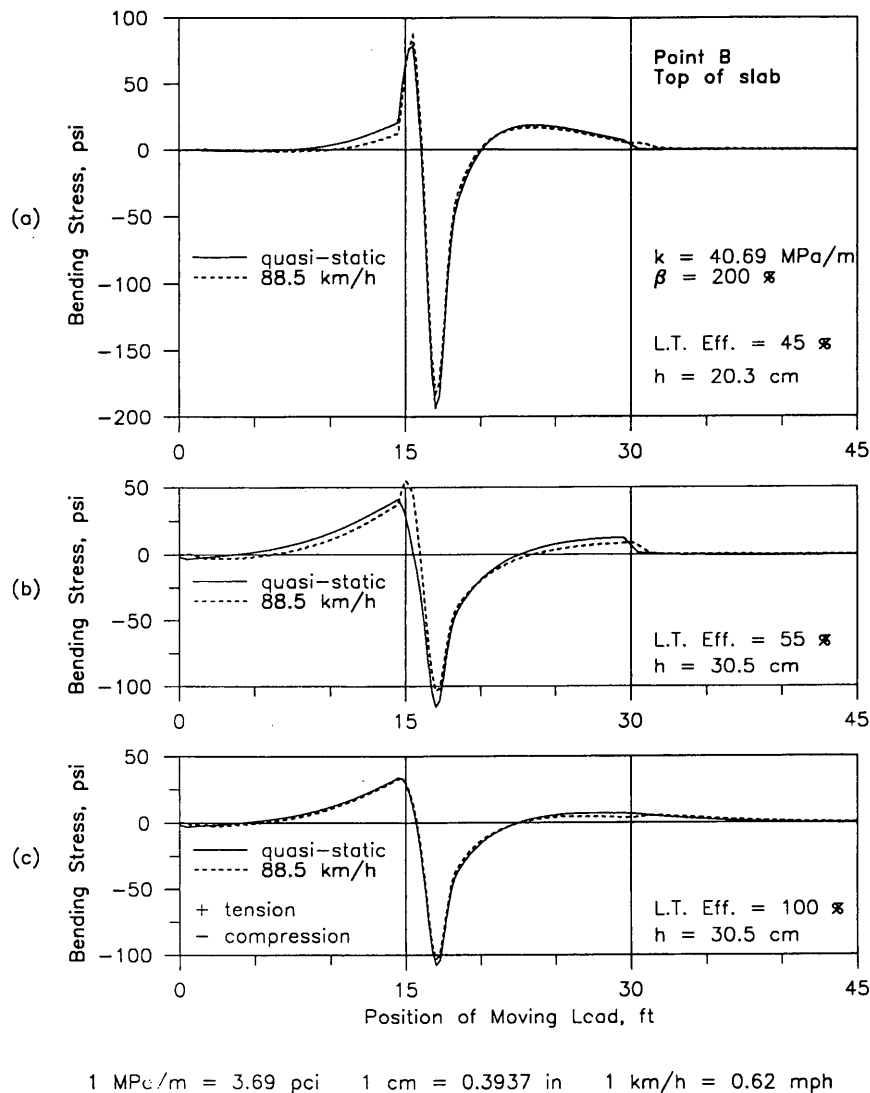
Figures 9 and 10 show the bending stress influence lines for points near the transverse joint and at midslab, respectively, due to a constant load moving at zero speed (quasistatic) and at 88.5 km/hr (55 mph) across a series of three 4.6-m (15-ft)-long slabs with

TABLE 1 Comparison of DYNA-SLAB Predictions with WES Experimental Results

Site No.	Foundation Parameters			Static Coeff. Subgrade Reaction, $k_s$ (MPa/m)	Maximum Deflection (mm)		
	Dynamic (15 Hz)		Damping Ratio, $\beta$		Measured	DYNASLAB	ILLISLAB
	Stiffness Coeff., $k$ (MPa/m)	Damping Coeff., $c$ (sec.MPa/m)					
1 <sup>a</sup>	-	-	-	-	-	-	-
3 <sup>b</sup>	20.3	0.36	1.33	81.3	0.132 0.212	0.137 0.197	0.146 0.209
7 <sup>c</sup>	8.9	0.34	2.74	22.2	0.203 0.329	0.238 0.349	0.509 0.748
11 <sup>d</sup>	42.5	0.48	1.03	21.9	0.070 0.099	0.055 0.078	0.121 0.172

1 mm = 39.37 mil      1 MPa/m = 3.69 pci

- <sup>a</sup>- unavailable data
- <sup>b</sup> Pensacola NAS: 10in PCC + 4in Base
- <sup>c</sup> Birmingham: 7in PCC
- <sup>d</sup> Sheppard AFB: 21in PCC + 6in Base



**FIGURE 9** Bending stress influence lines at Point B located along the top edge of the slab at 0.6 m from the transverse joint: (a) weak aggregate interlock; (b) dowel bars; (c) strong aggregate interlock.

different load transfer mechanisms and different thicknesses. A comparison between graphs (a) and (b) in both figures confirms that the effect of slab thickness is most important, whereas comparison of graphs (b) and (c) indicates that the effect of load transfer efficiency is minimal. More important for the present study, however, is the fact that both Figures 9 and 10 clearly show that the effect of vehicle velocity on bending stress response is negligible.

Figure 11 indicates that the effects of both vehicle velocity and load transfer efficiency on the deflection response are somewhat more pronounced than those on bending stress. In contrast, the effect of slab thickness on the deflection response is less noticeable than the effect on the bending stress response.

#### Effects of Pavement Roughness

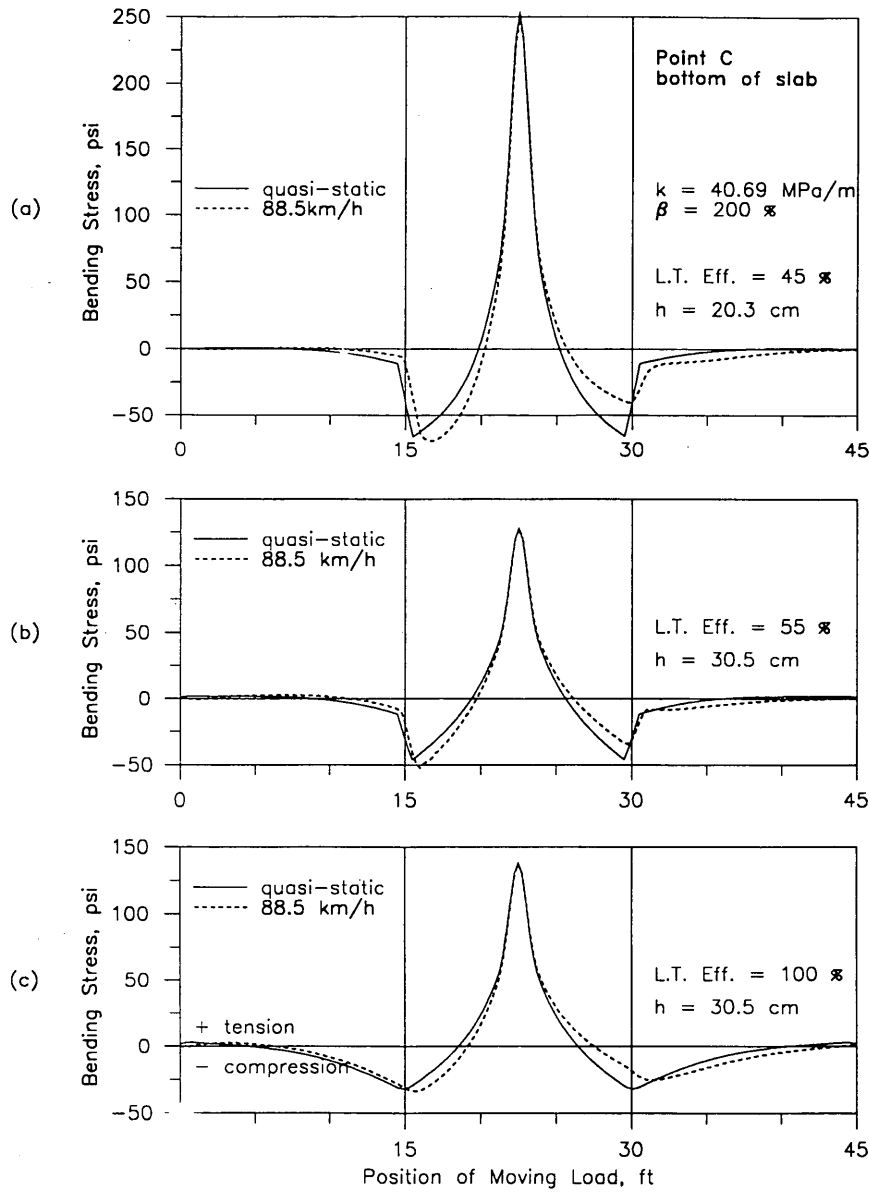
Dynamic wheel loads are caused by vibrations of the vehicle as it is excited by the roughness of the pavement surface. The dy-

amic forces generate additional stresses and strains in the pavement, which in turn may accelerate pavement deterioration and lead to increased truck "wear."

In the present study a truck simulation program termed VESYM, developed by Hedrick et al. (20), was used to generate axle loads. A typical 3-S2 18-wheel truck moving at 88 km/hr (55 mph) was assumed, and load time histories were generated for several surface profiles; these included faulting, day- and night-time warping, and breaks of different levels of severity. Breaks caused the most severe load increases and joint faulting produced larger peak dynamic axle loads than did warping, for realistic distress levels (13).

Figure 12 shows computed bending stress influence lines at critical points in the slab for different pavement roughnesses. The stress pulses caused by the five different axles have basically the same shape irrespective of the axle number or the distress type. This suggests that the response pulses are basically independent





1 MPa/m = 3.69 pci    1 cm = 0.3937 in    1 km/h = 0.62 mph

**FIGURE 10** Bending stress influence lines at Point C located along the bottom edge of the slab at midslab: (a) weak aggregate interlock; (b) dowel bars; (c) strong aggregate interlock.

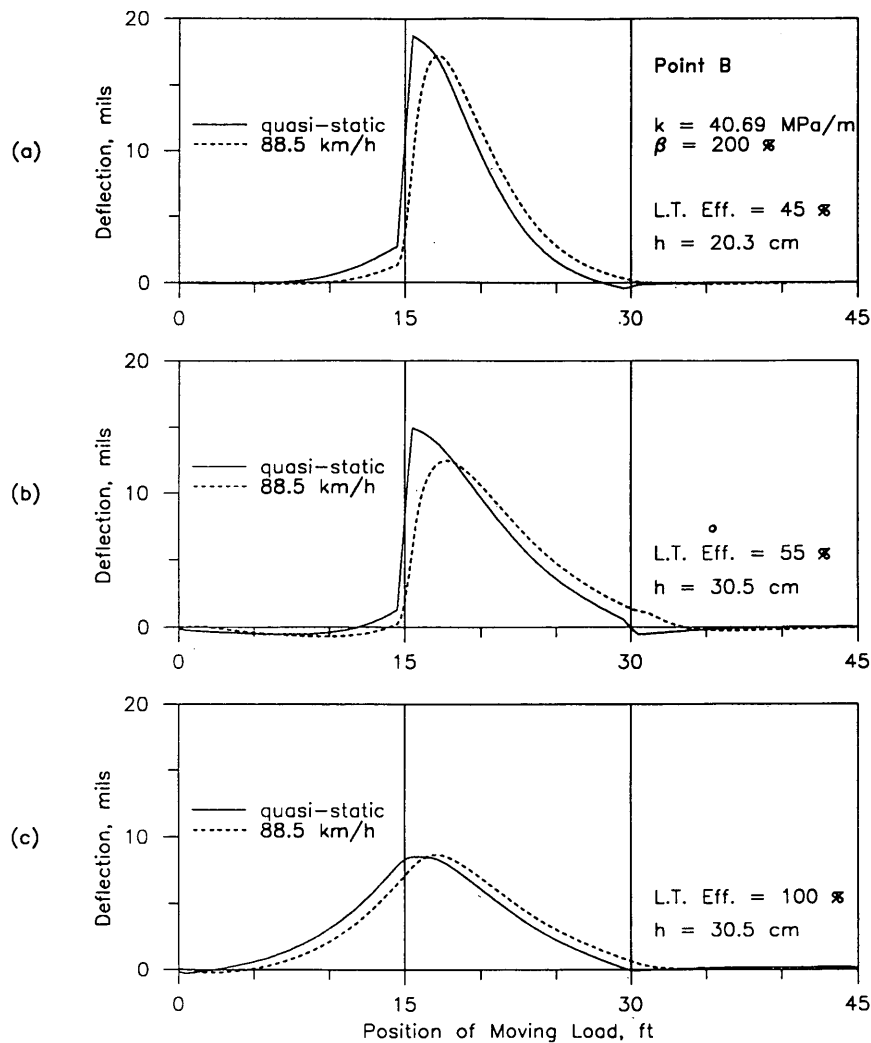
of the shape (frequency content) of the time histories of the axle loads. The frequency content of these pulses depend mainly on truck speed and other pavement factors such as the location of the response point, slab flexibility, or the load transfer mechanism. Furthermore, the quasistatic response curves are nearly identical to the dynamic curves (for  $\beta$  values of both 0.6 and 2.0). This is because the truck speed is considerably lower than the critical wave propagation velocity of the pavement.

These results clearly indicate that although it is important to correctly predict dynamic truck load histories in terms of their magnitudes and the locations of peaks (using truck simulation programs such as VESYM and appropriate pavement roughness

profiles), dynamic analysis is generally not needed to determine the response of concrete pavements. Instead, once the dynamic loads have been determined it is sufficient to use a quasistatic analysis in which moving loads have different time-dependent values at different positions on the pavement, but are otherwise assumed to be stationary and constant at each instant of time.

**Possibility of Dynamic Amplification due to Special Site Conditions**

The existence of a stiff layer (e.g., bedrock) at a relatively shallow depth [e.g., within 10 m (33 ft)] may amplify the pavement re-



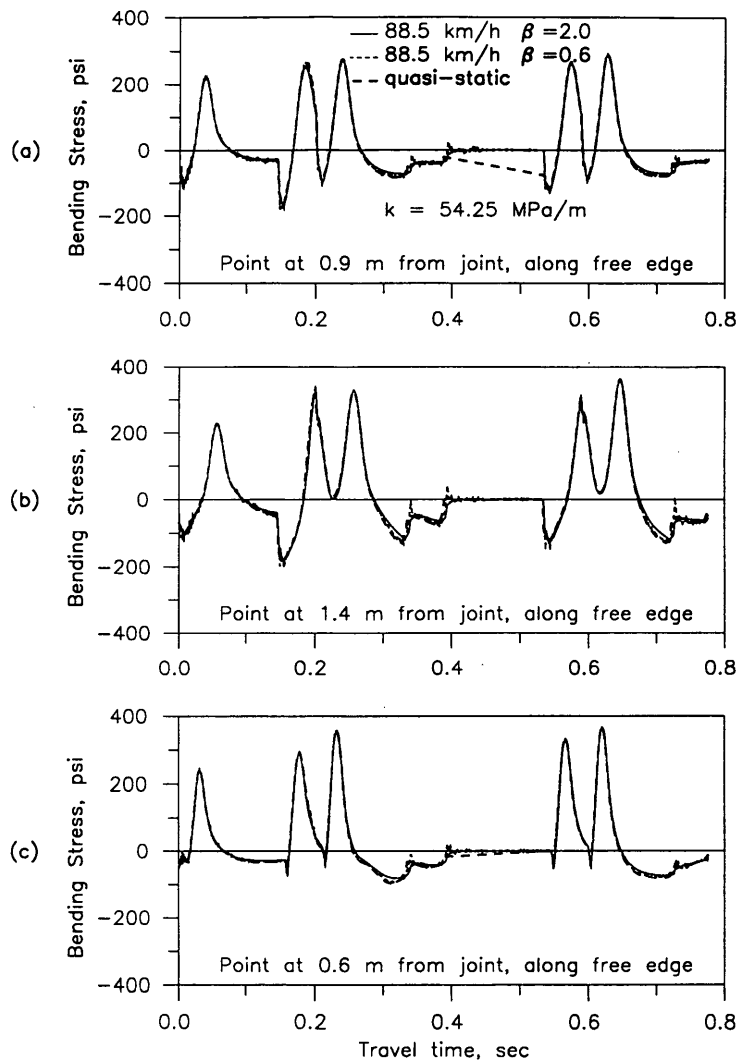
1 MPa/m = 3.69 pci    1 cm = 0.3937 in    1 km/h = 0.62 mph

**FIGURE 11** Deflection influence lines at Point B located along the edge of the slab at 0.6 m from the transverse joint: (a) weak aggregate interlock; (b) dowel bars; (c) strong aggregate interlock.

sponse at certain site-dependent frequencies as waves propagating away from the pavement slab reflect at the soil-bedrock interface and return back to the surface, interfering with downward propagating waves and, thus, increasing slab motions (resonance). In terms of foundation impedance coefficients, resonance occurs when the real part of the impedance (stiffness) is at or near a minimum. The possibility of resonant response because of a moving transient load was investigated in the present study for the hypothetical case in which both stiffness and damping vanish at a certain frequency. It was found that severe dynamic amplification (dynamic to static magnification factor higher than 5) will occur if the speed at which the load is moving causes a predominant frequency of the response that is nearly equal to the critical frequency (13). Further studies are needed to assess the practical significance of this finding.

## SUMMARY AND CONCLUSIONS

A new dynamic linear finite-element method has been presented for the analysis of jointed Portland cement-concrete pavements with different foundation supports and subjected to moving loads with arbitrary time histories. The method is formulated either in the time domain by using Newmark's constant average acceleration method (Winkler foundation only) or in the frequency domain by using the complex response method (both Winkler and layered viscoelastic solid foundations). A rational method for determining the dynamic foundation stiffness and damping coefficients for the Winkler foundation has been developed by using layered continuum theory. The models and methods used were verified by comparing computed results with available theoretical solutions and experimental results. Several examples have been presented to il-



1 MPa/m = 3.69 pci    1 cm = 0.3937 in    1 km/h = 0.62 mph

**FIGURE 12** Bending stress time histories at critical points in slab for different surface roughness profiles: (a) 0.5-cm warping; (b) 1-cm faulting; (c) 2.5-cm break.

illustrate the capabilities of the DYNA-SLAB computer program. The following conclusions were reached:

1. The major dynamic effect of moving traffic relates to the influence of vehicle speed and pavement roughness on the wheel loads that act on the pavement. Realistic time histories of wheel loads that consider pavement roughness and truck suspension characteristics can be determined by a truck simulation computer program. As far as the response of the pavement is concerned, only the peak values of the wheel loads and the velocity with which the loads traverse the pavement are important, with the latter being significant only in determining the durations and rise times of an individual pavement response pulse. The detailed frequency content of the wheel loads may be of importance for the

truck and its suspension system, but it appears to have little effect on the behavior of the pavement.

2. Once the dynamic wheel loads have been determined, there is generally little to gain from a complete dynamic analysis of the pavement and its foundation. It appears that a quasistatic analysis, in which the time histories of wheel loads are treated as sequences of stationary static loads, is sufficient and that results from this type of analysis will generally be slightly on the conservative side as far as design is concerned.

3. There exists a possibility that an amplifying resonance phenomenon would occur in pavements founded on sites with a reflecting rock surface at a relatively shallow depth. Additional studies will be required to establish the conditions under which this may occur. For these conditions dynamic analyses may be required for pavement design.

## ACKNOWLEDGMENTS

This research was made possible through funding provided by the University of California Transportation Center in collaboration with the U.S. Department of Transportation and the California Department of Transportation.

## REFERENCES

1. Tayabji, S. D., and B. E. Colley. *Analysis of Jointed Concrete Pavements*. Interim Report FHWA/RD-86/041. FHWA, U.S. Department of Transportation, Feb. 1986.
2. Chou, Y. T. *Structural Analysis Computer Programs for Rigid Multi-Component Pavements with Discontinuities—WESLIQUID and WES-LAYER*. Technical Reports 1, 2, and 3. Waterways Experiment Station, U.S. Army Corps of Engineers, Vicksburg, Miss., May 1981.
3. Tabatabaie, A. M., and E. J. Barenberg. Finite-Element Analysis of Jointed or Cracked Concrete Pavements. In *Transportation Research Record 671*, TRB, National Research Council, Washington, D.C., 1978, pp. 11–19.
4. Huang, Y. H. Finite Element Analysis of Slabs on Elastic Solids. *Journal of Transportation Engineering*, ASCE, Vol. 100, No. 2, 1974, pp. 403–416.
5. Huang, Y. H., and S. T. Wang. Finite Element Analysis of Concrete Slabs and Its Implications for Rigid Pavement Design. In *Highway Research Record 466*, HRB, National Research Council, Washington, D.C., 1973, pp. 55–69.
6. Chen, S. S. *The Response of Multi-Layered Systems to Dynamic Surface Loads*. Ph.D. dissertation. University of California, Berkeley, 1987.
7. Hanazato, T., K. Ugai, M. Mori, and R. Sakaguchi. Three-Dimensional Analysis of Traffic-Induced Ground Vibrations. *ASCE Journal of Geotechnical Engineering*, Vol. 117, No. 8, Aug. 1991.
8. Cebon, D. *An Investigation of the Dynamic Interaction Between Wheeled Vehicles and Road Surfaces*. Ph.D. dissertation. University of Cambridge, Cambridge, United Kingdom, 1985.
9. Kukreti, A. R., M. R. Taheri, and R. H. Ledesma. Dynamic Analysis of Rigid Airport Pavements with Discontinuities. *ASCE Journal of Transportation Engineering*, Vol. 118, No. 3, 1992, pp. 341–360.
10. Melosh, R. J. Basis for Derivation of Matrices for the Direct Stiffness Method. *Journal of the AIAA*, Vol. 1, No. 7, 1963, pp. 1631–1637.
11. Zienkiewicz, O. C., and Y. K. Cheung. The Finite Element Method for Analysis of Elastic Isotropic and Orthotropic Slabs. *Proc., Institution of Civil Engineers*, Vol. 28, Aug. 1964, pp. 471–488.
12. Tabatabaie, A. M. Dynamic Analysis of Pavement Systems-Model Evaluations. Presented at 70th Annual Meeting of the Transportation Research Board, Washington, D.C., 1991.
13. Chatti, K. *Dynamic Analysis of Jointed Concrete Pavements Subjected to Moving Transient Loads*. Ph.D. dissertation. University of California, Berkeley, 1992.
14. Bathe, K., and E. L. Wilson. *Numerical Methods in Finite Element Analysis*. Prentice-Hall, Englewood Cliffs, N.J., 1976.
15. Lysmer, J., M. B. Tabatabaie, R. Tajirian, S. Vahdani, and F. Ostadan. *SASSI—A System for Analysis of Soil-Structure Interaction*. Report 81-02, UCB/GT. University of California, Berkeley, April 1981.
16. Fryba, L. *Vibration of Solids and Structures Under Moving Loads*. Noordhoff International Publishing, Groningen, The Netherlands, 1972.
17. Boquet, D., and D. Le Houedec. Comportement d'une Chaussée Reponsant sur un Matelas Antivibratile et Soumise à des Charges Roulantes Vibratoires se Déplaçant à Vitesse Constante (in French). *Annales de l'Institut Technique du Bâtiment et des Travaux Publics, Paris, Série: Essais et Mesures*, March 1979, pp. 33–56.
18. Harr, M. E. Influence of Vehicle Speed on Pavement Deflections. In *Proc., Highway Research Board 41st Annual Meeting*, HRB, National Research Council, Washington, D.C., 1962, pp. 77–82.
19. Bentsen, R. A., A. J. Bush III, and J. A. Harrison. *Evaluation of Non-destructive Test Equipment for Airfield Pavements—Phase I: Calibration Test Results and Field Data Collection*. Technical Report GL-89-3. Waterways Experiment Station, U.S. Army Corps of Engineers, Vicksburg, Miss., Jan. 1989.
20. Hedrick, J. K., M. J. Markow, B. D. Brademeyer, and E. Abbo. *The Simulation of Vehicle Dynamics Effects on Road Pavements*. Final Report DTRS5684-C-0001. Office of University Research, U.S. Department of Transportation, Dec. 1988.

---

Publication of this paper sponsored by Committee on Rigid Pavement Design.